Egyptian Geophysical Society
EGS Journal, vol. 2, No. 1, 31-35 (2004)

ANALYSIS OF THE BOUGUER GRAVITY DATA OF NORTHWESTERN SINAI BASIN USING THE HORIZONTAL GRADIENT MAGNITUDE

S. O. Elkhateeb

Geology Dept., Qena Faculty of Science, South Valley Univ.

تحليل بيانات بوجير التثاقلية في حوض شمال غرب سيناء باستخدام حساب مقدار التدرج الأفقى

الخلاصة: يتناول هذا البحث تحليلاً لخريطة بوجير في حوض شمال سيناء من خلال حساب مقدار التدرج الأفقى فى الطريقة التثاقلية، وقد عولجت بيانات الخريطة باستخدام طريقة فيليبس (١٩٩٧) للتدرج الأفقى للعمق حيث تم تقدير مواقع وأعماق الطبقات وقد تبين من دراسة الخريطة أن تضاريس الصخور القاعدية كما لو أنها المصادر المسببة والتى تتمثل في هيئة تراكيب قبابية وارتفاعات مشابهة لتلك التى تنتمى إلى نظام القوس السورى المشاهد على السطح جنوب المنطقة ذات الأهتمام، كما أن العناصر التركيبية (الصدوع) توضح خطوطاً مغربية تسبب تعقيدات تركيبية مشابهة كثيراً للصدوع الممتدة على هيئة نسق درجية أو قطع من الصدوع المتجاورة، ومن ناحية أخرى فقد أظهرت تقديرات العمق ارتباط الأعماق الضحلة (٠,٥ كيلو متر) بالسطوح العليا للمصادر المسببة والتراكيب القبابية أما الأعماق الغائرة (٨ كيلو متر) فتحتل الأجزاء الشمالية والجنوبية الشرقية والجنوبية الغربية للمنطقة تحت الدراسة.

ABSTRACT: *The present work deals essentially with the analysis of the Bouguer gravity map of north Sinai basin via computing the horizontal-gradient magnitude (HGM). The data of the computed map has been processed using the horizontal-gradient depth analysis (HDEP), as implemented by Phillips (1997), where the locations and depths to layer edges were determined. Inspection of the resulted map exhibits the basement configuration as being a number of causative sources, domal structures and/or uplifts similar to those belonging to the Syrian arc system present at the surface to the south of the studied area. Also, structural elements (faults) exhibit arcuate strikes making structural complexities typical of extensional faulting such as en echelon and anastomosing fault segments. On the other hand, depth estimates showed that shallow depths approaching 0.5 km are associated with the tops of the interpreted causative sources and domal structures, whereas deep ones reaching 8.0 km occupy the northern, southeastern and southwestern parts of the area.*

INTRODUCTION

The study area lies in the northwestern part of Sinai Peninsula of Egypt; between lat. 30º and the Mediterranean sea shore N and the Suez Canal and 33º 35 E (Fig. 1). Geomorphologically, the area is featureless except the southeastern part in which the Maghara anticline is cropped out giving rise to elevated area trending NE-SW (Abu El-Ata, 1991). The geology of the area shows several units, according to Barakat (1982) a generalized lithostratgraphic column of northern Sinai beginning with the oldest is a sequence of strata of different ages that include: Triassic, Jurassic, Cretaceous, Tertiary and Quaternary.

The goal of this study is to map faults and igneous rocks within the basin-fill sediments. Mapping faults that offset rocks of the north Sinai basin helps delineate the lateral extent and subsurface geometry of different lithologic units and is important to understand the overall structural set up of the basin. Surface mapping of these faults is difficult due to widespread cover of eolian sand and colluvium. Drill-hole information provides a reasonable understanding of the subsurface conditions, However, this information is sparse and most of them lie outside the studied area.

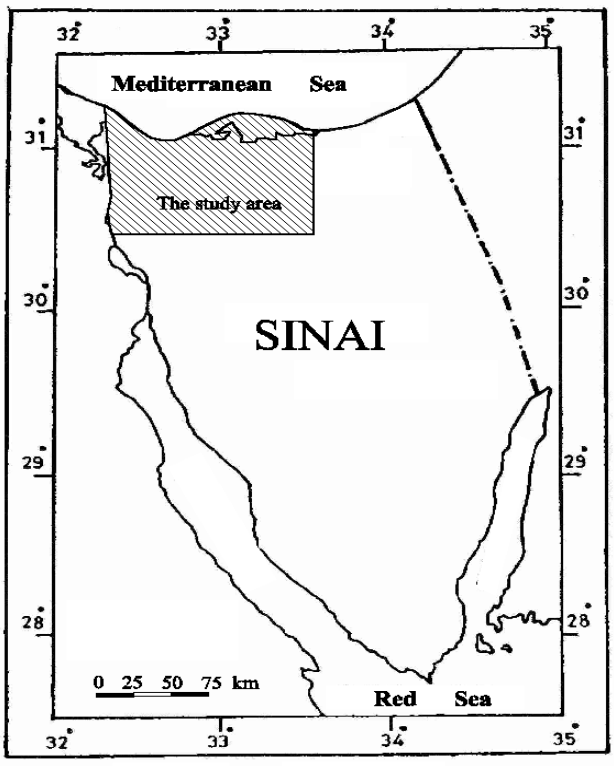

FIG. (1) LOCATION MAP OF THE STUDY AREA.

Several analytical techniques have been applied to locate geologic boundaries and contacts using gravity or magnetic data. Horizontal-gradient analysis of gravity data is a powerful tool that helps delineating the vertical and lateral locations of the edges of the target feature. Cordell (1979) and Cordell and Grauch (1985) used the maximum amplitudes of the horizontal gradients (without the vertical gradient) to locate near-vertical geologic boundaries from gravity or pseudogravity anomalies. In essence, the horizontal gradient method is a special case of the use of the analytic signal where the gravity anomaly is equivalent to the vertical magnetization anomaly from the same causative body through Poisson's relationship (Baranov, 1957). In this case, even if we do not add the vertical gradient in computing the amplitude of the analytic signal, in the absence of interference, the resulting amplitude (a bell-shaped function) also has its maximum value directly over the abrupt boundaries (Nabighian, 1972).

Implementation

The Bouguer anomaly map of the study area Fig. (2) has been reproduced from the original map compiled by the General Petroleum Corporation in 1986 by digitizing along the contour lines. The obtained data file was firstly gridded and contoured to ensure the validity of the previous steps by reproduction of the original map. Then, applying Fourier transformations, the horizontal derivative of both the x and y directions have been computed from the original data grid. Finally, the horizontal gradient magnitude (HGM) has been computed as representing the root of the square sum of both the horizontal derivatives (i.e. the amplitude of the horizontal derivatives) and the resulted data grid is then contoured as shown in Fig. (3). On the other hand, in order to infer the information contained in this map in a readable manner horizontal-gradient depth (HDEP) analysis, as implemented by Phillips (1997), has been carried out where the locations of and depths to layer edges were determined. The analysis makes use of the technique published firstly by Blakely and Simpson (1986) for locating the horizontal positions of magnetic contacts from gridded magnetic data. Their approach was based on the observations of Cordell and Grauch (1985) that the magnitude of the horizontal gradient of the pseudogravity transformation of a magnetic field peaks over vertical magnetic contacts. In the automated method, a 3x3 window is passed over the horizontal gradient magnitude (HGM) grid, and an attempt is made to fit parabolic peaks to the four 3-point scans passing through the center of the window. If a sufficient number of peaks is found (usually 2 to 4), the location of the largest peak is taken as the contact location. The technique has been applied to the grid of the computed horizontal gradient magnitude and the resulted strikes of and depths to the causative sources were shown in Fig. (4).

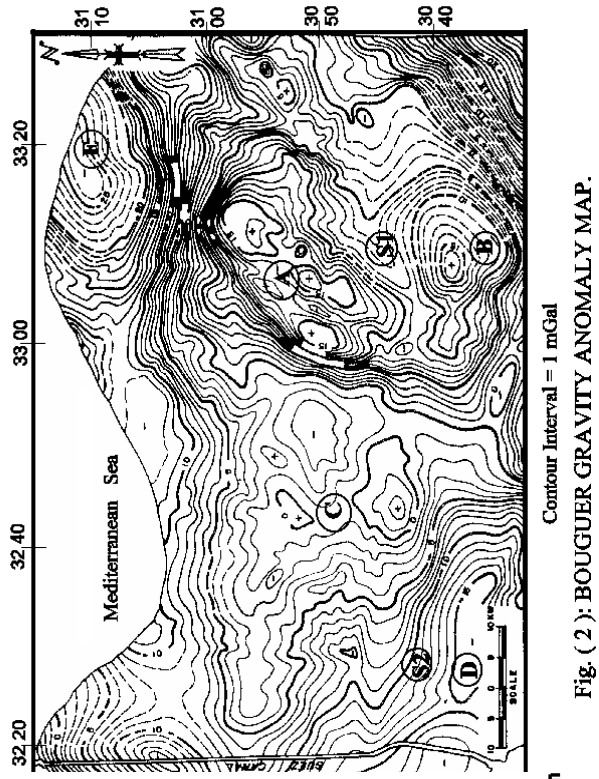

Fig. (2): BOUGUER GRAVITY ANOMALY MAP.

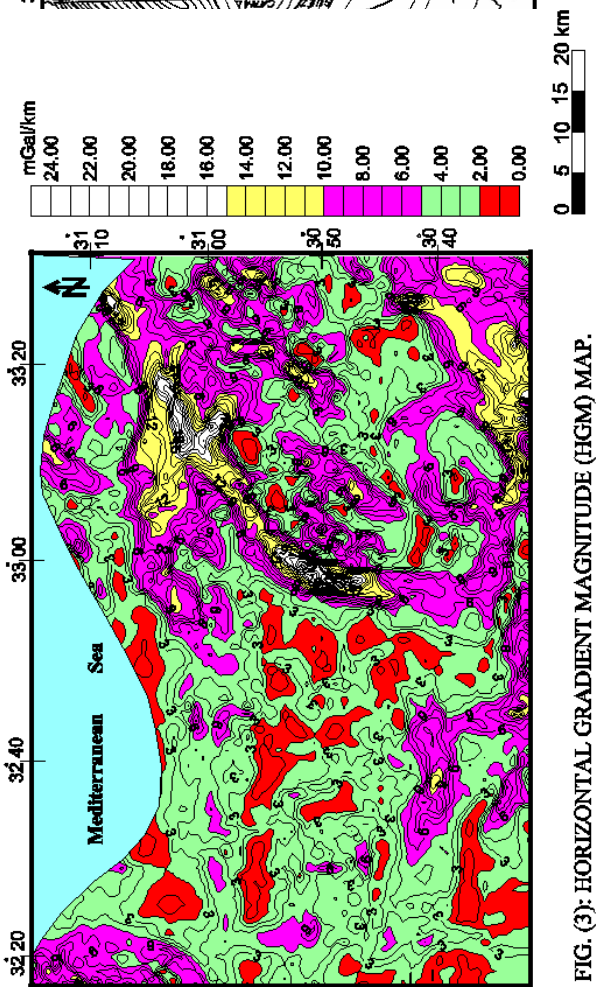

FIG. (3): HORIZONTAL GRADIENT MAGNITUDE (HGM) MAP.

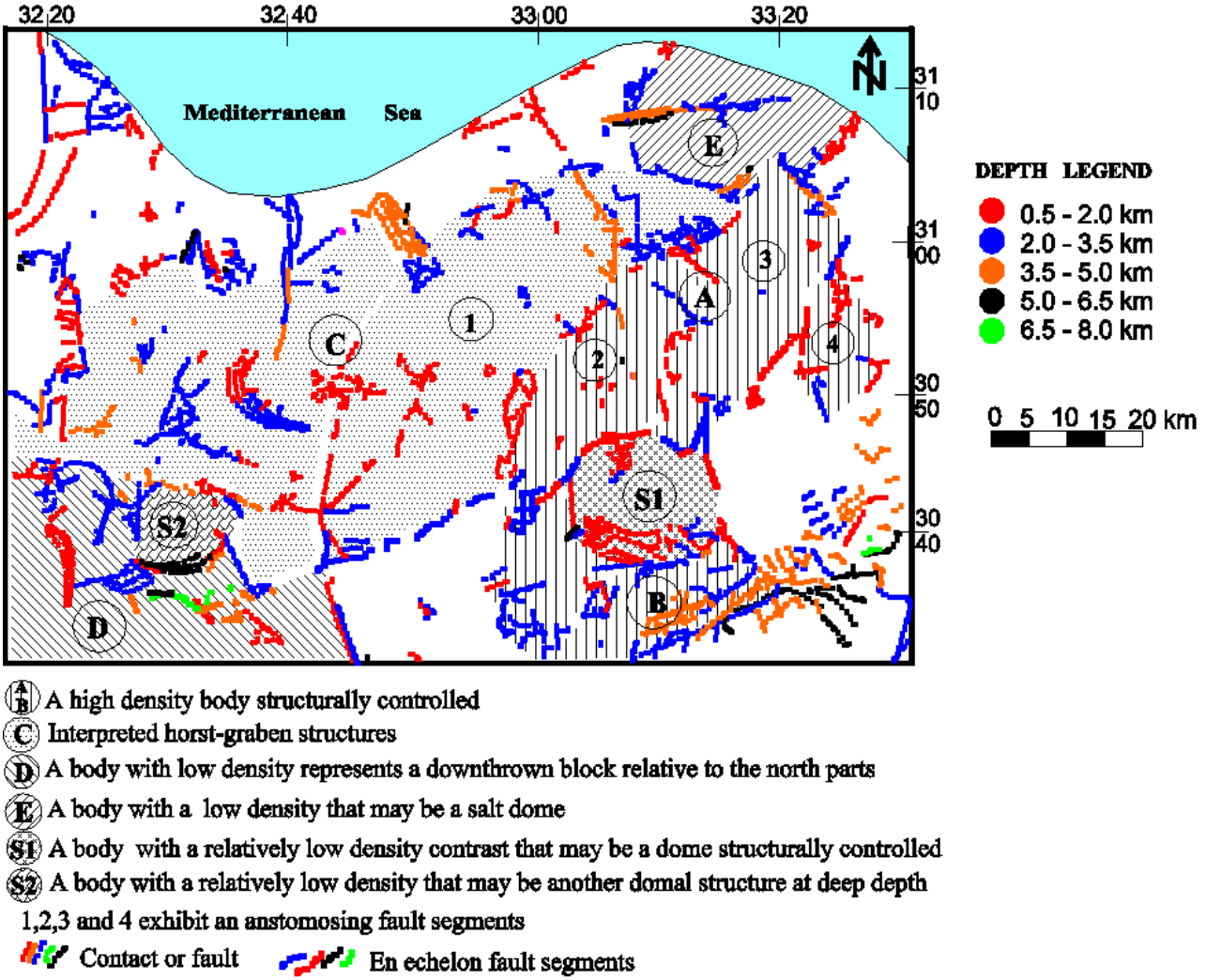

FIG. (4): HORIZONTAL GRADIENT LOCATION - DEPTH MAP (HGLD).

DISCUSSION

The Bouguer Gravity Map

The Bouguer map of the study area Fig. (2) shows a number of parts that exhibit different gravity signatures. The eastern portion is manifested by two positive gravity belts. The first belt marked (A) on the map aligned nearly in NE-SW direction with some extension at its extreme northeastern part to the east; meanwhile it is separated from it by a steep gradient trending in the same direction. The second belt denoted as (B) lies to the south and aligned in an E-W direction. The two belts are followed to the southeast by a steep gravity gradient oriented NE-SW. The western portion denoted as (C) is separated from the eastern one by a steep gradient trending NNE-SSW. It is formed of a number of negative anomalies intervening with other positive ones and followed to the southwest through a high gradient by a negative anomaly part showed on the map as (D) oriented WNW-ESE. The extreme northern part of the area is occupied by an E-W trending belt of negative anomalies that is separated from the southern parts by a pronounced high gradient zone. The most conspicuous anomaly lies in the northeastern part of the map and denoted as (E).

The Horizontal Gradient Magnitude (HGM) Map

Horizontal-gradient analysis of gravity data generally delineates the vertical and lateral locations of the subsurface causative sources; hence, it provides a view of the overall pattern of faulting, which aids in understanding the structural and tectonic framework of the basin.

To identify fault expressions, results of horizontal-gradient analysis of north Sinai basin gravity data are presented as shown in Fig. (3). Mapping local maxima of the horizontal-gradient magnitude (HGM) of gravity data has been used to locate fault traces and other near-vertical contacts. In map view, faults are presumed to produce a single alignment, or one "track" of prominent HGM maxima. However, multiple HGM tracks may be

found, in such a case, each track is associated with a side of the faulted block (Grauch et. al., 2001).

The Horizontal Gradient Location-Depth (HGLD) Map

No crystalline basement outcrops are present in the study area, which is overlain by a sequence of sediments that generally thicken towards the north and the west. Structure within the basement is suspected to strongly influence the location of faulting within the sedimentary cover. The locations of the top edges of offset layers are indicated by the strikes plotted from HDEP analysis of the HGM map. As expected, the strikes conform to the ridges of maxima on the gravity HGM map from which it was computed. They also delineate other alignments of gradient maxima that are harder to delineate on the HGM map. In map view lithological variations in the basement are emphasized on the HGLD map Fig. (4) as linear anomalies showing a variety of structural patterns. In particular, towards the southeastern part, a major circular feature can be identified as a possible domal structure where also conformable arcuate trends are apparent out from the center of this structure. Also, another circular feature with a limited ariel extent has been outlined at the southwestern portion exhibiting arcuate trends and deep depths giving an impression of a second small-scale domal structure. The whole structure is then affected by numerous fault sets that exhibit structural complexities, of which the more prominent is the en echelon arrangement of the NE trending fault segments that resulted from the dissection of this fault by the NS trending set of faults; also an anastomosing fault segments are very well developed as great blocks oriented in the same trend as the causative NE trending faults. The fault lines assume NW, NE, NS and EW directions. The cross-cut relations of these faults are obvious in different parts, in the northeast a conspicuous NW set that is cut by a prominent NE trending fault and the whole swarm has been offset by a NS trending fault.

Depth estimates at the location of the HGM maximum are estimated by exploiting the relations between the HGM, the horizontal distance from the maximum, and the depth that is expected for a vertical contact (Roest and Pilkington, 1992). Overall, the depth estimates as seen from the HGLD map show a range of values that seem plausible with the configuration of the outlined causative sources, domal structures and/or uplifts. It is obvious that shallow depth values approaching 0.5 km are concentrated above the tops of the outlined high-relief structures whereas the deep ones reaching 8 kms are deviated outwards especially in the southeastern, northern and southwestern parts. It deserves mention to note that depth estimates over the suggested domal structures exhibit a high gradient relief towards the southeastern flanks in comparison to the northwestern ones, this conclusion is in close agreement with similar structures outcropping on the surface to the south of the study area (Said, 1962). It is of paramount importance to note that about 93 % of the estimated depths fall between 1.5 and 7.7 km and the relatively shallow and deep depth estimates represent only about 5.3 % and 1.7 % respectively. So, we must take into consideration that some part of the estimated shallow depths less than 1.5 km represent artifacts and may be the result of short wavelengths introduced as a consequence of the used interpolation technique.

Inspection of this map (HGLD) in conjunction with the Bouguer one shows a close conformity since the interpreted causative sources from the first map are fair reflections of pronounced anomalies in the original Bouguer map. However, a glance on both maps Figures 2 and 4 shows the following:

1- The positive two anomaly belts defined as (A) and (B) in the Bouguer map are outlined as one causative source of high-density, structurally controlled and separated into some parts as a result of faulting.

2- The western portion marked as (C) and represented by a number of intervening low and high anomalies in the Bouguer map is reflected as an alternation of horst-graben structures extending approximately in NE-SW direction.

3- The negative anomaly part denoted as (D) in the Bouguer map appeared as a body extended in E-W direction possessing high-gradient relief and deeply seated.

4- The negative anomaly (E) in the extreme northeastern portion of the Bouguer map is very well resolved as a structurally controlled body with low-density that may have an extension in the sea, it is suggested to be a salt dome. Its shape is a witness.

The previously suggested domal structures (S1 and S2) show a faint gravity expression in the Bouguer map; meanwhile, they are very well developed as domal structures in the HGLD map giving rise to the conclusion that these structures may be the result of faulting.

Generally, we can say that most of the structural elements in the form of faults exhibit an arcuate nature strongly related to the syrian arc system present in these areas. Also, most of the outlined causative sources are structurally controlled.

CONCLUSION

Based on the analysis of the constructed horizontal gradient magnitude map Fig. (3) where the locations of and depths to layer edges were determined Fig. (4) the subsurface geological and structural picture of north Sinai basin was inferred. The subsurface features can be imagined as consisting of a number of causative

sources, domal structures and/or uplifts of various natures. The eastern part of the study area is represented by a major emerging body extending in nearly NE direction and including

in its center a domal structure that seems to be formed as a result of structural control. The extreme northeastern and southwestern corners appeared as structurally controlled bodies of low densities that may be either domal structures or downfaulted blocks. The western part was reflected in an alternation of horst-graben structures oriented generally in NE-SW direction. On the other hand, most of the structural elements (faults) exhibit an arcuate pattern assuming trends more or less parallel to those present at the south of the study area and belongs to the prominent syrian arc system; it seems that these faults were responsible for the formation of the shore line. Also, some structural patterns typical of extensional faulting, such as en echelon and anastomosing fault segments were formed. Finally, the depth estimates show a range of values from 0.5 - 8.0 km. Shallow depths are concentrated above the central parts of the area whereas the deep ones approximating 8.0 km. are deviated outwards especially in the northern, southeastern, and southwestern parts.

Within the frame of the applied method and the results obtained it seems that utilizing modern geophysical techniques is robust in the interpretation of potential field data. The method demonstrates the high efficiency and improvement of the detection of geologic boundaries and their depths rather than conventional old methods.

REFERENCES

Abu El-Ata, A. S. A, Rizkalla, R. I., and Abdel Hady, A. I., 1991, The role of wave number filtering in the separation of the residual and regional gravity anomalies of northwestern Sinai peninsula, Egypt: E.G.S. Proc. of the 9th Ann. Meet., Cairo, pp. 19-42.

Barakat, M. G., 1982, General review of petroliferous provinces of Egypt with special emphasis on their geologic setting and oil potentialities: Pet. And Gas Proj., Cairo Univ., M.I.T., 86.

Baranov, V.,1957, A new method for interpretation of aeromagnetic maps: Pseudogravimetric anomalies: Geophysics, 22, 359-383.

Blakely, R. J., and Simpson, R. W., 1986, Locating edges of source bodies from magnetic or gravity anomalies: Geophysics, 51, 1494-1498.

Cordell, L., 1979, Gravimetric expression of graben faulting in Santa Fe country and the Espanola Basin, New Mexico: New Mexico Geol. Soc. Guidebook, 30th Field Conf., 59-64.

Cordell, L., and Grauch, V. J. S., 1985, Mapping basement magnetization zones from aeromagnetic data in the San Juan Basin, New Mexico, in Hinze, W. J., Ed., The utility of regional gravity and magnetic anomaly maps: Soc. Explor. Geophys., 181-197.

El-Eraqi, M. A. F., 1992, Magnetic interpretation and modelling of northern Sinai area: Proc. 3rd Conf. Geol. Sinai Develop., Ismailia, 37-42.

General Petroleum Corporation, Egypt, 1986: Exploratory report to the compilation gravity iso-anomaly map of Egypt,Cairo.

Grauch, V. J. S., Hudson, M. R., and Minor, S. 2001, Aeromagnetic expression of faults that offset basin fill, Albuquerque Basin, New Mexico, Geophysics online, 15 Jan., 2001.

Nabighian, M. N., 1972, The analytic signal of two-dimensional magnetic bodies with polygonal cross-section: Its properties and use for automated anomaly interpretation: Geophysics, 37, 507-516.

Phillips, J. D., 1997, Potential-field geophysical software for the PC, version 2.2: U.S. Geological Survey Open-File Report, 97-725, 34p.

Roest, W. R., Verhoef, Jacob, and Pilkington, Mark, 1992, Magnetic interpretation using the 3-D analytic signal: Geophysics, 57, 116-125.